

Competition for charge compensation in borosilicate glasses: Wide-angle x-ray scattering and molecular dynamics calculations

L. Cormier*

Laboratoire de Minéralogie-Cristallographie, Universités Paris 6 et 7 et Institut de Physique du Globe de Paris et UMR CNRS 7590, 4 place Jussieu, 75252 Paris Cedex 05, France

D. Ghaleb and J.-M. Delaye

CEA/DCC, Service de Confinement des Déchets, CEA Valrho-Marcoule, BP 171, 30207 Bagnols/Céze Cedex, France

G. Calas

Laboratoire de Minéralogie-Cristallographie, Universités Paris 6 et 7 et Institut de Physique du Globe de Paris et UMR CNRS 7590, 4 place Jussieu, 75252 Paris Cedex 05, France

(Received 3 November 1999)

Wide-angle x-ray scattering (WAXS) has been used to investigate the structure of complex sodium (aluminum) borosilicate glasses containing four, five, and six oxides. WAXS data were compared with previous molecular dynamics calculations on these glasses. Small differences were observed which are mainly due to a smaller Si-O distance in the models (1.58 Å) compared to the experimental distance (1.60 Å). These discrepancies were removed by slightly moving the atomic positions using the reverse Monte Carlo code. Changes in the first cation-oxygen distances were sufficient to give an excellent fit of the WAXS data, with little modification of the medium range structure. This allows a determination of the structural features observed in the correlation functions and a validation of the numerical simulations for complex multicomponent glasses. The dependence of the glass structure on its chemical composition is discussed.

I. INTRODUCTION

The structure of multicomponent silicate glasses is based on a polymeric network with coexisting cations, which may act as modifiers or as charge-compensating cations needed for balancing the charge deficit of oxygen neighbors. This situation occurs, for instance, when trivalent cations are substituted to silicon in the polymeric network. Glass properties may be strongly affected, depending if cations are network modifiers or charge compensators. This has been shown in alkali-oxide-bearing glasses in which transport properties are strongly affected by the substitution of silicon by aluminum, in correlation with important structural modifications.¹ Borosilicate glasses are a good example of materials in which cations may occur in the two situations. These glasses are of great interest in a wide range of applications, such as electronics, materials science, waste management, etc. One of their peculiar structural properties comes from the ability of boron to occur in three or four coordination, depending on its possibility to get charge compensation from the coexisting cations. However, the complex chemical composition makes the correlation functions difficult to interpret beyond the first coordination shell, in the absence of structural models. We have investigated the competition for charge compensation

between different highly charged cations, boron, aluminum, and zirconium in borosilicate glasses that have been previously investigated by Raman spectroscopy² and for which molecular dynamics (MD) models have been proposed.³

The direct determination of the glass structure by wide-angle x-ray scattering (WAXS) has been combined with molecular dynamics calculations, allowing us to decipher the various pair contributions to the total correlation function. We show that the sodium environment is modified when aluminum is present and that aluminum and zirconium compete favorably against tetrahedral boron for charge compensation.

II. SAMPLE AND EXPERIMENT

A. Sample preparation

Three glasses have been selected, a sodium borosilicate glass (four-oxide glass), with the additional presence of alumina (five-oxide glass), and further addition of calcium oxide (six-oxide glass). The composition of these glasses is reported in Table I. The sodium (and calcium) oxide content has been chosen to be lower than needed for ensuring a full compensation of the charge deficit due to highly charged

TABLE I. Compositions (mol %) of the four, five, and six-oxide glasses and experimental densities d .

	SiO ₂	B ₂ O ₃	Na ₂ O	ZrO ₂	Al ₂ O ₃	CaO	$d(\text{g cm}^{-3})$
four oxides	67.25	17.41	13.55	1.79			2.415
five oxides	64.13	16.81	13.27	1.78	4.01		2.479
six oxides	60.12	16.00	12.64	1.70	3.82	5.72	2.510

cations if all boron atoms were in tetrahedral coordination. Glasses were prepared by mixing reagent grade oxides. The powders were melted at 1100 °C. The melts were poured on graphite crucibles and annealed at 520 °C during 1 h.

B. Wide-angle x-ray experiment

Glass samples have been cut as slabs of 3 cm diameter and 4 mm thick. WAXS measurements were performed on a diffractometer equipped with Mo K α radiation and a bent graphite monochromator (Philips, PW1729). The intensity measurements were carried out by the $\theta/2\theta$ step scanning method and in the angular range $0.5^\circ < 2\theta < 140^\circ$, which corresponds to a Q range from 0.8 to 16.6^{-1} (and $Q = |\mathbf{Q}| = 4\pi \sin \theta / \lambda$ is the scattering vector, 2θ is the scattering angle, and λ is the radiation wavelength). The total counts accumulated at each measured point was not less than 20 000. The x-ray source was operating at a current of 35 mA and an accelerating voltage of 50 kV.

The measured x-ray scattering intensities were corrected for polarization and absorption factors. The normalization constant is determined by both the Krogh-Moe-Norman's method⁴ and the high-angle method.⁵ The incoherent scattering intensity was calculated with the analytical formulas given by Balyuzi.⁶ After correction and normalization, the coherently scattered intensity per atom, $I_{coh}(Q)$, is used to calculate the total structure factor $S(Q)$,

$$S(Q) = [I_{coh}(Q) - \langle f^2(Q) \rangle] / \langle f(Q) \rangle^2, \quad (2.1)$$

in which $\langle f \rangle$ and $\langle f^2 \rangle$ are the mean and the mean-square scattering factors, respectively, calculated from analytical expressions⁷ and corrected for anomalous dispersion.⁸ By Fourier transforming the reciprocal-space data, we obtain the total correlation function $G(r)$,

$$G(r) = 2/\pi \int_0^{Q_{max}} Q [S(Q) - 1] \exp(-\alpha Q^2) \sin(Qr) dQ \\ = 4\pi r \rho_0 (g(r) - 1), \quad (2.2)$$

where $g(r)$ describes the local-density fluctuations around unity and ρ_0 is the average number density. The $\exp(-\alpha Q^2)$ is a modification function used to down-weight the high-angle data, with the damping factor $\alpha = 0.005$. The $S(Q)$ function is a weighted sum of all the partial structure factors $S_{\alpha\beta}(Q)$,

$$S(Q) = \sum_{\alpha, \beta} W_{\alpha\beta}(Q) S_{\alpha\beta}(Q) \quad (2.3)$$

with the weighting factors

$$W_{\alpha\beta}(Q) = \frac{c_\alpha c_\beta \Re(f_\alpha(Q, E) f_\beta^*(Q, E))}{|\langle f(Q, E) \rangle|} (2 - \delta_{\alpha\beta}), \quad (2.4)$$

where c_i and f_i are the atomic fraction and the atomic scattering factor for atoms of type i , respectively. The dependency of f_i with the scattering vector Q and the x-ray energy E leads to a convolution in the real space between the Fourier transforms of the weighting factors and the partial pair distribution functions (PPDF's) $G_{\alpha\beta}(r)$,

$$G(r) = \sum_{\substack{\alpha\beta \\ \beta > \alpha}} TF(W_{\alpha\beta}) * g_{\alpha\beta}(r). \quad (2.5)$$

Considering Eq. (4), dilute (small c_α) or light elements (small f_α) have a small weighting factor and make negligible contribution to the WAXS data. The dominant PPDF's to the $G(r)$ function in the investigated glasses are Si- α and O- α pairs.

III. COMPUTATIONAL METHODS

A. Molecular dynamics calculations

The molecular dynamics (MD) procedure used to investigate the structure of the four, five, and six-oxide glasses have been presented in previous papers³ and only a brief account will be given below. The three systems contain 5184 atoms in a cubic box according to the glass compositions and the experimental densities given in Table I. The atomic interactions were simulated using the Born-Mayer-Huggins potentials completed by three-body terms to constrain some local angles (O-Si-O, Si-O-Si, and O-B-O). A very strong constrain was applied on the O-B-O angles in order to obtain a fraction of four-coordinated boron atoms which is consistent with experimental values. Some macroscopic quantities (Na diffusion constant, thermal expansion coefficient) determined for the models showed good agreement with experimental results.³

B. Reverse Monte Carlo simulations

Reverse Monte Carlo (RMC) technique was used to improve the analysis of the experimental spectra.⁹ RMC simulations have been used with success to extract three-dimensional atomic models in quantitative agreement with the experimental data.^{1,10} The fit consists of minimizing the squared difference between the experimental and calculated structural factors by moving atoms randomly. In this procedure, distances of closest approach between two types of atoms are imposed and silicon and aluminum are constrained to occur in tetrahedral sites.

IV. RESULTS AND DISCUSSION

A. Reciprocal-space functions

The structure factors of the three borosilicate glasses extend up to 14 \AA^{-1} , with a good signal-to-noise ratio [Fig. 1(a)]. The three spectra are similar at high Q values. In this region, the signal mainly arises from the contribution of Si-O, B-O, and Al-O pairs, which are not expected to change significantly with the glass composition. Some differences are seen on the position and shape of the first peak, around 2 \AA^{-1} , which is related to the medium range structure of the glass (5–15 \AA). The peak position shifts down by 0.2 \AA^{-1} in the five and six-oxide glasses, in which the width is smaller. This suggests a better medium range organization of these glasses, compared to the four-oxide glass.

B. Real-space functions

The total correlation functions [Fig. 1(b)] show several well-defined peaks up to 6 \AA . Beyond the first intense peak

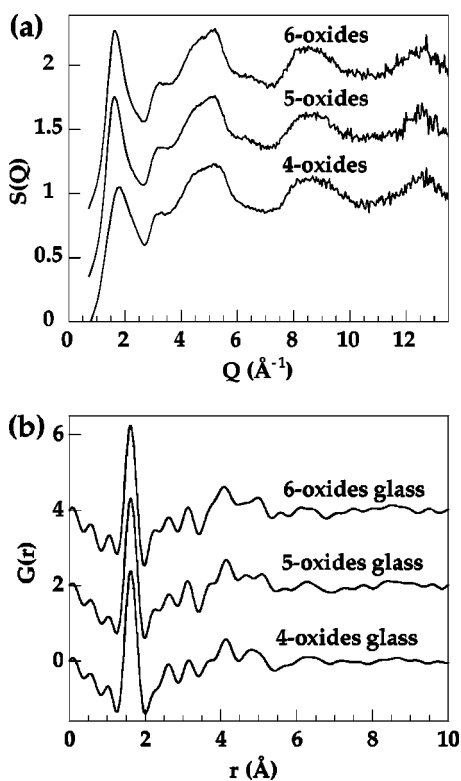


FIG. 1. (a) Wide-angle x-ray structure factors $S(Q)$ and (b) total correlation functions $G(r)$.

located near 1.62 \AA , corresponding to the overlap of the first B-O, Si-O and, if present, Al-O distances, some differences appear in the position and relative intensity of the structural features. Although it is impossible at this stage to determine the origin of these peaks, it appears that the four-oxide glass has a less-defined structure than the two other glasses, as predicted from a qualitative examination of the structure factors. The interpretation of such a complex correlation function may only be conducted by using atomic models.

C. Comparison between experiments and simulations

We have used the PPDF's derived from the MD models calculated for these glasses.³ When these functions are weighted according to the expressions (3) to (5), a direct comparison may be performed between the experimental and simulated structure factors and total correlation functions (Fig. 2). When considering the structure factors, there is a good agreement above 3 \AA^{-1} , with a strong disagreement on the peak at low Q . A double peak is predicted by MD while only a single peak is experimentally observed. In addition, it is worth noting that this low- Q peak is shifted towards higher- Q values in the four-oxide glass relative to the two other glasses. If there is a general agreement between the predicted and observed total correlation functions up to 6 \AA , some differences exist in the position and intensity of the various features. For instance, the first, intense peak is slightly shifted down by 0.03 \AA in the MD models. We have used the RMC method to determine the origin of these discrepancies, using MD models as the starting configuration. An agreement in the position and intensity of the peaks in the experimental and calculated data is obtained after only

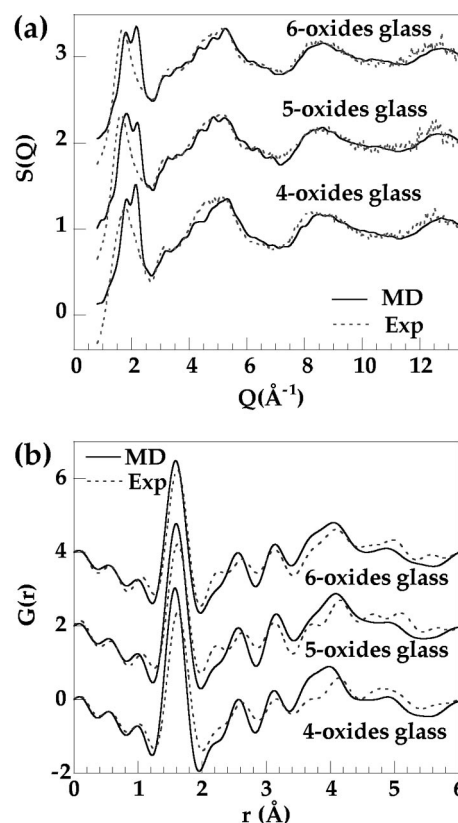


FIG. 2. Comparison between (a) the structure factors and (b) the total correlation functions for the x-ray experimental data (dotted curves) and the molecular dynamics calculations (solid curves). The correlation functions were obtained by Fourier transforming the structure factors calculated from the MD models, with a truncation at $Q = 13.5 \text{ \AA}^{-1}$. Some curves are displaced for clarity.

20 000 accepted moves among 100 000 tried moves (Fig. 3). These values are lower by at least two orders of magnitude as compared to RMC calculations starting with a random configuration, indicating that only a few atomic changes are needed to adjust the MD models to the experimental data.

Among the network formers, aluminum is found in tetrahedral sites. A more complex figure is observed for boron. In the starting configuration derived from MD calculations, the fraction of tetrahedrally coordinated boron, $^{[4]}\text{B}$, has been fixed at 67%, a value derived from previous ^{11}B NMR studies on sodium borosilicate glasses.¹¹ After the RMC fits [Fig. 4(a)], the three models show a lower proportion of $^{[4]}\text{B}$ (calculated with a cutoff B-O distance of 2.1 \AA), the six-oxide glass presenting the lowest content (Table II). A similar proportion of $^{[4]}\text{B}$ has been recently found in aluminoborosilicate glasses, in which ^{11}B NMR data indicate a decreasing proportion of $^{[4]}\text{B}$ with increasing alumina content.¹² Recent ^{11}B NMR data¹³ obtained for the four, five, and six-oxide glasses show good agreement with the simulations except for the five-oxides glass (Table II). This discrepancy may be due to the small weights of the partials involving boron and hence the difficulty to constrain the B-O pair. When alumina is added to the five-oxides glass, Na are charge compensating the $(\text{AlO}_4)^-$ tetrahedra first, which lead to the conversion of some $(\text{BO}_4)^-$ units present in the four-oxide glass into BO_3 units in the five-oxides glasses. In the six-oxides glass, Ca^{2+} can charge balancing two

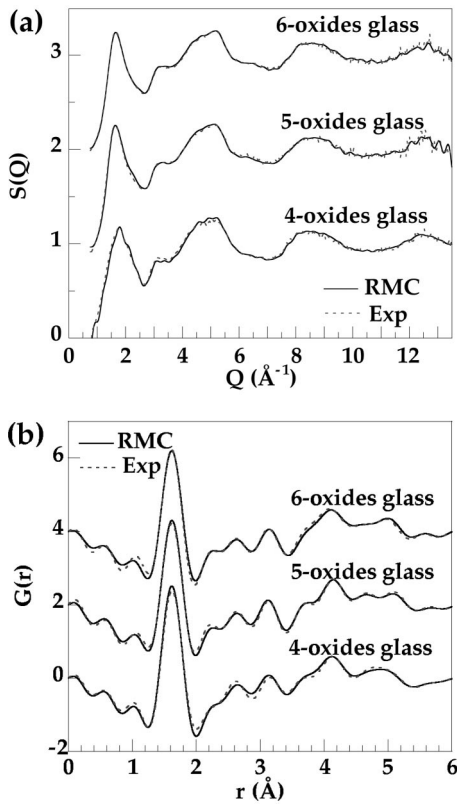


FIG. 3. Comparison between (a) the structure factors and (b) the total correlation functions for the x-ray experimental data (dotted curves) and the models after the RMC fits (solid curves). The correlation functions were obtained by Fourier transforming the structure factor S calculated from the RMC models, with a truncation at $Q = 13.5 \text{ \AA}^{-1}$. Some curves are displaced for clarity.

$(\text{AlO}_4)^-$ and more Na^+ are thus available for charge-compensating $(\text{BO}_4)^-$ units, which explains the higher proportion of ^{14}B in the six-oxides glass than the five-oxides glass. These results indicate the higher ability of aluminum to be in tetrahedral sites compared to boron. Another highly charged cation, zirconium, occurs in sixfold coordination. The Zr-O distances found in the RMC models are in good agreement with Zr K -edge extended x-ray absorption fine-structure (EXAFS) studies of these glasses, 2.10 and 2.08 \AA , respectively.¹⁴ MD models predict Zr-O distances of 2.15 \AA [Fig. 4(b)], an indication that the Zr-O potential needs to be adjusted to agree with the experimental values. The zirconium surrounding is not affected by the presence of aluminum or calcium, and this element retains its charge-compensating cations at the expense of boron which partly remains in triangular, uncompensated sites.

The understanding of the sodium surrounding has been improved by RMC models, as Na-O distances derived from MD calculations are too large by 0.2–0.3 \AA than the experimental data. An important difference between the glasses concerns the first Na-O distances which are larger by 0.4 \AA in the four-oxide glass than in the two other glasses. In the former, only one Na-O shell is found, centered at 2.6 \AA , a value similar to that found in crystals. By contrast, the latter exhibit a bimodal distribution, with contributions at 2.20 and 2.55 \AA [Fig. 4(c)]. A similar splitting has been observed in a sodium tetrasilicate glass, in which the first peak in the

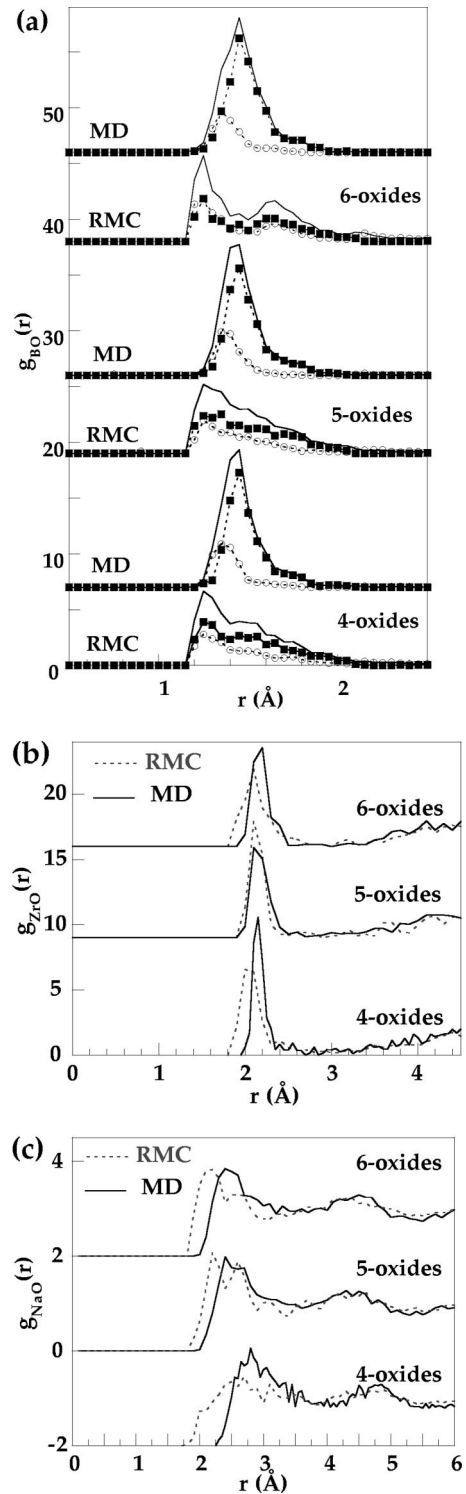


FIG. 4. Comparison between the pair partial distribution functions calculated by MD (solid curves) and RMC (dotted curves). (a) B-O pair, showing the contribution for the three- (dotted-dashed curves) and four- (square-dashed curves) coordinated boron atoms (^{13}B and ^{14}B); (b) Zr-O pair; (c) Na-O pair.

Na-O PPDF obtained by a RMC modeling of neutron scattering data shows two separate Na-O distances, due to bonding to nonbridging (2.29 \AA) and bridging (2.45 \AA) oxygens.¹⁵ However, as aluminoborosilicate glasses do contain only few nonbridging oxygens (<10%), the larger Na-O distances may be attributed to the presence of sodium

TABLE II. Proportions of $^{[3]}\text{B}$ and $^{[4]}\text{B}$ in the four, five, and six-oxides glasses calculated from the RMC models, with a cutoff B-O distance of 2.1 Å, and compared with NMR results (Ref. 13).

	RMC $^{[3]}\text{B}(\%)$	models $^{[4]}\text{B}(\%)$	NMR $^{[3]}\text{B}(\%)$	data $^{[4]}\text{B}(\%)$
four oxides	42.2	57.8	39.2	60.8
five oxides	41.3	58.7	62.4	37.6
six oxides	53.7	46.3	54.0	46.0

atoms charge-compensating network forming aluminum or boron atoms. Similar distances have actually been observed in Na-bearing crystalline phases: in three-dimensional frameworks, such as feldspars, the shortest Na-O distances are 2.5–2.6 Å, whereas Na-O distances as short as 2.3 Å are observed in less polymerized silicate and borate crystals. Na coordination number N is in agreement with this interpretation: $N=8$ in the RMC model of the investigated glasses and 7–9 in three-dimensional framework silicates, while lower coordination numbers ($N=5$) are found in depolymerized silicate and borate crystals. A further indication is given by the decrease of Si and B neighbors when alumina is present, from 6.6 to 5.7 for Na-Si and from 3.7 to 3.1 for Na-B, respectively. This result is consistent with sodium atoms charge balancing aluminum at the expense of boron. Similar differences between a network modifying and charge-compensating role have been recently found for other cations, including lithium and strontium.^{1,16}

The medium range organization of the polymeric network has been investigated using ring statistics. The structure con-

sists mainly of five, six, and seven-membered rings. There are no significant changes after the RMC fits, which indicate that the alumino-borosilicate network is consistent with MD calculations. In addition, the percentage of nonbridging oxygens remains unchanged, lower than 10%, after RMC fits. The small number of nonbridging oxygens indicates an almost fully polymerized network that incorporates tetrahedrally coordinated aluminum and boron atoms, charge compensated by sodium and calcium. Octahedrally coordinated zirconium is linked to this network, as predicted from EXAFS studies on these glasses, and is also associated with charge-compensating sodium. As the structure of the polymeric network remains unchanged with the addition of alumina and lime, the incorporation of network-forming aluminum is compensated by the transformation of $^{[4]}\text{B}$ into $^{[3]}\text{B}$, ensuring a constant proportion of network formers. Additional studies on selective coupling between the various glass components are now in progress.

V. CONCLUSIONS

Coupling WAXS experiments and MD and RMC modelings allow the determination of atomic models consistent with the experimental data. The structure of complex alumino-borosilicate glasses and, in particular, the local surrounding of the various glass components can be described. Aluminum is preferentially incorporated in the polymeric network at the expense of boron. It is then possible to determine relative preferences for charge compensation between the various highly charged cations. This will allow a better prediction of physical properties of these important glass-forming systems.

*Author to whom correspondence should be addressed. Electronic address: cormier@lmcj.jussieu.fr

¹L. Cormier, P.H. Gaskell, G. Calas, J. Zhao, and A.K. Soper, *Phys. Rev. B* **57**, 8067 (1998).

²B. Boizot, G. Petite, D. Ghaleb, B. Reynard, and G. Calas, *J. Non-Cryst. Solids* **243**, 268 (1999).

³J.-M. Delaye and D. Ghaleb, *J. Non-Cryst. Solids* **195**, 239 (1996); *Mater. Sci. Eng., B* **37**, 232 (1996); J.-M. Delaye, V. Louis-Achille, and D. Ghaleb, *J. Non-Cryst. Solids* **210**, 232 (1997).

⁴J. Krogh-Moe, *Acta Crystallogr.* **9**, 951 (1956); N. Norman, *ibid.* **12**, 670 (1957).

⁵F. Marumo and M. Okuno, in *Material Science of the Earth Interior*, edited by I. Sunagawa (Terra Scientific, Tokyo, 1984), p. 25.

⁶H.H.M. Balyuzi, *Acta Crystallogr., Sect. A: Cryst. Phys., Diffr., Theor. Gen. Crystallogr.* **31**, 600 (1975).

⁷D.T. Cromer and J.B. Mann, *Acta Crystallogr., Sect. A: Cryst. Phys., Diffr., Theor. Gen. Crystallogr.* **24**, 321 (1968).

⁸S. Sasaki, KEK Report No. 88-14, 1989 (unpublished).

⁹R.L. McGreevy, *Nucl. Instrum. Methods Phys. Res. A* **354**, 1 (1995).

¹⁰L. Cormier, G. Calas, and P.H. Gaskell, *J. Phys. C* **9**, 10 129 (1997).

¹¹W.J. Dell and P.J. Bray, *J. Non-Cryst. Solids* **58**, 1 (1983).

¹²G. El-Damrawi, W. Müller-Warmuth, H. Doweidar, and I. A. Gohar, *Phys. Chem. Glasses* **34**, 52 (1993).

¹³B. Boizot (private communication).

¹⁴L. Galois, J.M. Delaye, D. Ghaleb, G. Calas, M. LeGrand, G. Morin, A. Ramos, and F. Pacaud, in *Scientific Basis for Nuclear Waste Management XXI*, edited by I. G. McKinley and C. McCombie, MRS Symposia Proceedings No. 506 (Materials Research Society, Pittsburgh, 1998), pp. 133–139; L. Galois, E. Pellegrin, M.-A. Arrio, P. Ildefonse, and G. Calas, *J. Am. Ceram. Soc.* **82**, 2219 (1999).

¹⁵N. Zotov and H. Keppler, *Phys. Chem. Miner.* **25**, 259 (1998).

¹⁶L. Cormier, G. Calas, S. Creux, P.H. Gaskell, B. Bouchet-Fabre, and A.C. Hannon, *Phys. Rev. B* **59**, 13 517 (1999).